Density Functional Complete Study of Hydrogen Bonding between the Water Molecule and the Hydroxyl Radical ($H_2O \cdot HO$)

ZHENGYU ZHOU,[1,2] YUHUI QU,[1] AIPING FU,[1] BENNI DU,[1] FAXIN HE,[1] HONGWEI GAO[1]

[1]*Department of Chemistry, Qufu Normal University, Shandong, Qufu 273165, People's Republic of China*

[2]*State Key Laboratory Crystal Materials Shandong University, Shandong, Jinan 250100, People's Republic of China*

Received 11 September 2001; accepted 14 April 2002

DOI 10.1002/qua.10315

ABSTRACT: The hydrogen bonding complexes formed between the H_2O and OH radical have been completely investigated for the first time in this study using density functional theory (DFT). A larger basis set 6-311++G(2*d*,2*p*) has been employed in conjunction with a hybrid density functional method, namely, UB3LYP/6-311++G(2*d*,2*p*). The two degenerate components of the OH radical $^2\Pi$ ground electronic state give rise to independent states upon interaction with the water molecule, with hydrogen bonding occurring between the oxygen atom of H_2O and the hydrogen atom of the OH radical. Another hydrogen bond occurs between one of the H atoms of H_2O and the O atom of the OH radical. The extensive calculation reveals that there is still more hydrogen bonding form found first in this investigation, in which two or three hydrogen bonds occur at the same time. The optimized geometry parameter and interaction energy for various isomers at the present level of theory was estimated. The infrared (IR) spectrum frequencies, IR intensities, and vibrational frequency shifts are reported. The estimates of the $H_2O \cdot OH$ complex's vibrational modes and predicted IR spectra for these structures are also made. It should be noted that a total of 10 stationary points have been confirmed to be genuine minima and transition states on the potential energy hypersurface of the $H_2O \cdot HO$ system. Among them, four genuine minima were located. Int J Quantum Chem 89: 550–558, 2002

Key words: density functional theory; hydrogen bonding; hydroxyl radical; water molecule

Correspondence to: Z. Zhou; e-mail: zhengyu@qfnu.edu.cn

Introduction

Molecular complexes are common in molecular science. A great amount of experimental and theoretical information has become available [1–11]. Many hydrogen-bonded complexes between the water molecule and other molecules have been reported in the literature [12–14]. The $H_2O \cdot HO$ system has been the subject for the study of hydrogen bonding due to its importance in atmospheric chemistry, catalytic reactions, energy transfer, and biologic processes. The hydrogen-bonded system between the water molecule and the OH radical have been first studied theoretically by Schaefer et al. [15, 16] (see structures **1–3** and **6–9**) using various *ab initio* molecular orbital (MO) methods, in which the highest level employed was CISD, with DZP or TZ2P basis sets. Wang et al. [17] report partly the study on the $H_2O \cdot HO$ system using a density functional theory (DFT), with a larger basis set 6-311++G(2*d*,2*p*) (see structures **1–3** and **6**), verifying that structure 3 is transition state at the B3LYP/6-311++G(2*D*,2*P*) level. However, this does not constitute a complete study of the potential energy hypersurface by using DFT because the hydrogen bond could be formed in another way.

The $H_2O \cdot HO$ system is different from all hydrogen-bonded systems characterized to date in that there are two electronic states. The origin of these two distinct states, of course, lie with the doubly degenerate $^2\Pi$ state of the OH radical. The $C_{\infty\nu}$ point group of the isolated OH radical is reduced to C_s symmetry as OH approaches the water molecule. The two degenerate components of the $^2\Pi$ state split into distinct states. The characterization of the distinct states of the $H_2O \cdot HO$ system should be an important challenge. In the complete DFT study on the $H_2O \cdot OH$ system, several features of the current study are as follows: (1) One genuine minima and two transition states were first located using DFT; (2) vibrational modes of three stationary points newly found in this work are analyzed; (3) the fundamentals vibrational frequencies of genuine minima are partly predicted. The interaction energies and predicted infrared (IR) spectrum for these structures are reported in an attempt to act as a guide for future experimental investigations of $H_2O \cdot OH$ complexes.

Theoretical Approach

A variety of theoretical methods have been used in the research, including the unrestricted Hartree–Fock (UHF) method, the unrestricted second-order Møller–Plesset theory (UMP2), as well as the hybrid density functional methods, which are UBLYP, UB3LYP, UB1LYP, and UG96LYP [18, 19]. It has been shown that DFT can give a proper reproduction of the experimental data for the molecular structure and vibrational IR spectrum of H_2O and OH. The basis sets applied were 6-311++G(2*d*,2*p*) and 6-311++G(3*df*,2*p*). These basis sets have been successfully used in the studies of the properties of many hydrogen bond complexes with a reasonable small basis set superposition error [20]. DFT had been demonstrated to be an effective method for the study of electronic structures and vibration properties of molecular complexes [21–23]. All molecular geometries were fully optimized using the 6-311++G(2*D*,2*P*) basis set at the UB3LYP level of theories mentioned above. At the same level of theory, the IR spectra—including vibration frequencies, vibration modes, and IR intensities—were obtained via analytic second derivative methods to determine the nature of different stationary points. The total energy was also calculated. The interaction energy for the $H_2O \cdot HO$ complexes were considered as the differences between the total energies of the complexes and the separated monomers at infinite distance. The single-point energy calculations were done using the unrestricted coupled cluster method including single and double excitation and perturbational estimates of the effects of connected triple excitation [CCSD(T)] [24], which have been shown to predict energies more reliably [25]. The zero-point vibration energy (ZPE, $1/2 \sum h\omega_1$) correction and thermal correction (TC) at 298.15 calculated at the UB3LYP/6-311++G(2*D*,2*P*) level were employed. Because both $^2A'$ and $^2A''$ electronic states of the $H_2O \cdot HO$ complex are acquired, it will need to alter the initial orbital configurations in the C_s symmetry with the GUESS = ALTER option implemented in Gaussian 94. The symmetry of the corresponding electronic state can be identified directly through the optimized orbital configurations, and so do both $^2B_1$ and $^2B_2$. The number of imaginary frequency (0 or 1) confirms whether a local minimum or a transition state has been located. In addition, all transition states were subjected to internal reaction coordinate (IRC) [26, 27] calculations at the same level of

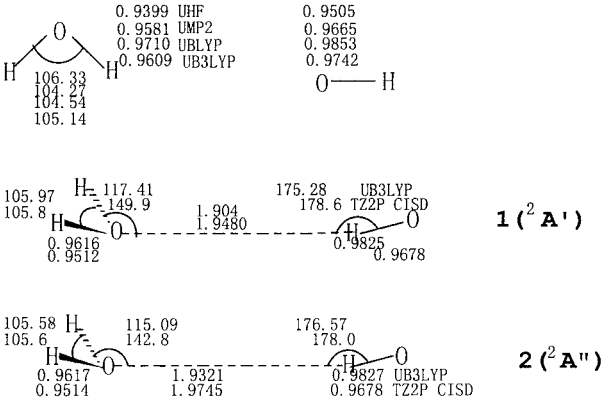

FIGURE 1. Theoretical geometries for structures **1** (*A′*) and **2** (*A″*). Bond lengths are in Å and bond angles are in degrees. The values of the lower line are from Ref. [16].

theory to verify that we have the correct transition state for the reaction when we examine the structures that are downhill from the saddle point and to facilitate connection between the reactants and products. Each IRC terminated upon reaching a minimum using the default criterion. All calculations were performed with the Gaussian 94 package [28].

Results and Discussion

EQUILIBRIUM GEOMETRIES AND INTERACTION ENERGIES

The optimized structures for $H_2O \cdot OH$ complexes are shown in Figures 1–5. The total energies and the interaction energies for various $H_2O \cdot HO$ isomers at the UB3LYP/6-311++G(2*D*,2*P*) level of theory are listed in Table I. The interaction energies, including ZPE scaling and TC at 298.15 K, are also presented. For structures **1** and **2** (Fig. 1), the water molecule and hydroxyl radical exhibit hydrogen bonding between the O (in H_2O) and H (in OH) ($H_2O\cdots HO$), depending on the orientation of the singly occupied orbital as the OH radical ($^2\Pi$ state) approaches the H_2O; structures **1** and **2** belong to $^2A'$ and $^2A''$ electronic states, respectively. Because these two states ($^2A'$ and $^2A''$) have been studied extensively in Refs. [16] and [17], those will be discussed briefly here. According to Figure 1, the geometry parameters of structures **1** and **2** are slightly larger than those of the monomers H_2O and OH. In addition, the $O\cdots HO$ bond angle is almost linear; both structures have similar geometric parameters except for the distance of the hydrogen bond, which in structure **1** ($^2A''$) is 0.0281 Å longer than that in structure **2** ($^2A'$) at the UB3LYP/6-311++G(2*D*,2*P*) level of theory. Accordingly, structure **1** has smaller interaction energy than structure **2** (see Table I). The highest level of theory in this article, i.e., UB3LYP/6-311++G(2*D*, 2*P*), predicts the interaction energy of the $^2A'$ state to be 24.43 kJ/mol and that of the $^2A''$ state to be 22.93 kJ/mol.

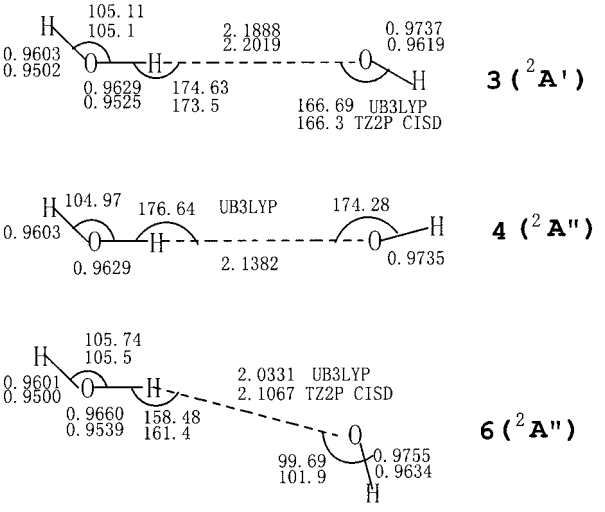

FIGURE 2. Theoretical geometry for structures **3**, **4**, and **6**. Structures **3** (*A′*) and **4** (*A″*) are transition states. Bond lengths are in Å and bond angles are in degrees. The values of the lower line are from Ref. [16].

When hydrogen bonding occurs between the H atom (in H_2O) and the O atom (in OH), one obtains different structures (see Fig. 2). It can be observed from Figure 2 that the resulting complexes are structures **3**, **4**, and **6** with C_S symmetry. It is noteworthy that the conclusions in Figure 2 are different from Refs. [16] and [17]. We confirm that both structures **3** and **4** are transition states. Depending on the

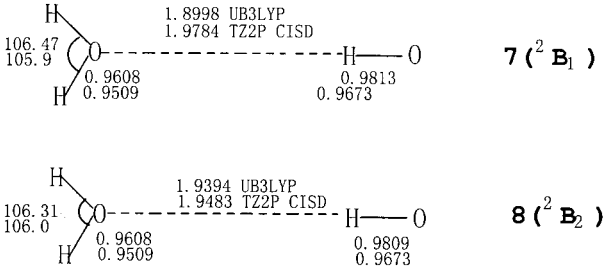

FIGURE 3. Theoretical geometry for structures **7** (B_1) and **8** (B_2). Bond lengths are in Å and bond angles are in degrees. The values of the lower line are from Ref. [16].

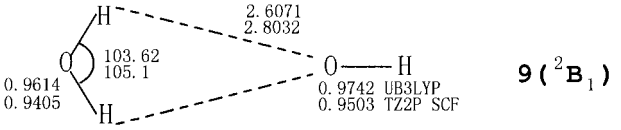

FIGURE 4. Theoretical geometry for structure **9** (B_1), which is not a transition state. Bond lengths are in Å and bond angles are in degrees. The values of the lower line are from Ref. [16].

orientation of the singly occupied orbital as the OH radical ($^2\Pi$ state) approaches the water molecule, these two states are characterized as $^2A'$ (structure **3**, with in-plane singly occupied orbital) or $^2A''$ (structure **4**, with out-of-plane singly occupied orbital). Both are transition states with different geometries, the critical difference between them lying with the orientation angle of H···OH and O—H···O. Contrary to structures **3** and **4**, structure **6** is a genuine minimum characterized as $^2A''$. It can be seen from inspection of Figure 2 that the largest qualitative difference between $^2A''$ and $^2A'$ equilibrium geometry lies with the H···OH orientation and OH···O orientation angles. The H···OH angle is 166.69° and 174.28° in structures **3** and **4**, respectively. And, the intermolecular angle (OH···O) of structure **3** is somewhat smaller than that of structure **4**. It is in general held that the most critical structural parameter is the H···O hydrogen bond length, shown by Figure 2 to be 2.1888 Å for structure **3** ($^2A'$) in the excited state and 2.1382 Å for structure **4** ($^2A''$) in the ground state. Therefore, interaction energy of structure **4** is slightly (0.83 kJ/mol) larger than those of others. In comparison with structures **3** and **4**, structure **6** is more bent and bond length is shorter than structures **3** and **4**; in fact, structure **6** is about 5.44 kJ/mol lower in energy because of the existence of single π-type hydrogen bonds between O—H (in the OH radical) and the lone pair on the O atom of H_2O, in addition to primary σ-type hydrogen bond [29]. Just as for structures **1** and **2**, it can be seen from Figure 3 that the possible structures **7** and **8** possess C_{2V} symmetry; there are also two electronic states depending on the orientation of the singly occupied orbital as the OH radical (in $^2\Pi$ state) approaches the water molecule. These two states are characterized as $^2B_2$ (structure **8**, with in-plane singly occupied orbital) and $^2B_1$ (structure **7**, with out-of-plane singly occupied orbital). From Figure 3, it can be observed that the predicted geometric parameters of the two structures are almost the same except for the hydrogen bond distance. The correlation of the H···O distance with the interaction energy also can be seen from the two structures. The H···O distance of structure **7** is ~ 0.04 Å shorter than that of structure **8** at the UB3LYP/6-311++G(2*D*,2*P*) level of theory. Accordingly, this state exhibits stronger hydrogen bonding and larger interaction energy. Actually, the energy splitting between structures **7** and **8** is small (only ~ 1.92 kJ/mol) (see Table I). In comparison with structures **3**, **4**, and **6**, structures **7** and **8** are about 8–12 kJ/mol lower in energy, so they are more likely to be observed.

There is another reasonable form of hydrogen bonding for this system, in which the water molecule donates two equivalent hydrogen bonds to the two lone pairs of the oxygen atom in OH moiety

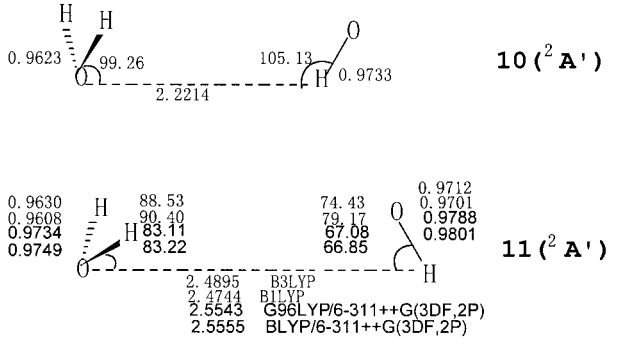

FIGURE 5. Theoretical geometry for structures **10** and **11**. Structure **10** is a transition state. Bond lengths are in Å and bond angles are in degrees.

TABLE I

Total energies (in hartree) and interaction energies E_{int} (in kJ/mol)[a] of different isomers of $H_2O \cdot OH$.

Species	Total energies	Interaction energies
1 ($^2A'$)	−152.2356686	−24.44 (−7.45)[b]
2 ($^2A''$)	−152.2350967	−22.93 (−5.65)
3 ($^2A'$)	−152.229564	−8.41 (+0.96)
4 ($^2A''$)	−152.2298916	−9.25 (−0.71)
6 ($^2A''$)	−152.2319881	−14.77 (−2.01)
7 ($^2B_1$)	−152.2354789	−23.93 (−11.17)
8 ($^2B_2$)	−152.2347371	−22.01 (−9.50)
9 ($^2B_1$)	−152.2292372	−7.53 (−2.39)
10 ($^2A'$)	−152.2330888	−17.66 (−6.74)
11 ($^2A'$)	−152.2337773	−19.46 (−2.89)
CCSD(T)//B3LYP	−151.9274037	−11.35 (−0.52)
$H_2O + \cdot OH$	−152.2263632	0.0
CCSD(T)//B3LYP	−151.9230793	0.0

[a] $E_{int} = E_{complex} - \Sigma E_{monomers}$.
[b] Values in parentheses have included the ZPE and TC at 298.15 K.

TABLE II

Harmonic vibrational frequencies (in cm^{-1}) and IR intensities (in parentheses, in km/mol) of $H_2O \cdot OH$.

Species	ω_1	ω_2	ω_3	ω_4	ω_5	ω_6	ω_7	ω_8	ω_9
1	173.5	182.7	196.3	431.1	645.7	1639.5	3561.8	3815.6	3916.1
	(89.4)	(1.3)	(92.4)	(200.9)	(143.4)	(74.6)	(342.8)	(16.2)	(91.6)
2	175.5	198.1	207.9	546.7	547.2	1643.4	3558.6	3814.6	3912.8
	(23.4)	(0.8)	(174.9)	(161.9)	(162.7)	(73.5)	(330.9)	(16.1)	(87.9)
3	81.4	116.5	−164.3	232.8	369.9	1651.3	3722.7	3808.8	3911.8
	(73.1)	(25.1)	(193.6)	(123.4)	(100.2)	(63.8)	(24.3)	(57.5)	(110.7)
4	−217.7	6.2	114.2	163.8	385.9	1646.9	3728.4	3811.1	3912.3
	(179.1)	(23.9)	(0.0)	(44.0)	(197.8)	(67.5)	(26.6)	(53.2)	(110.8)
6	101.3	111.2	165.6	293.9	396.9	1648.8	3704.9	3748.6	3898.4
	(175.4)	(136.5)	(78.4)	(263.7)	(3.1)	(54.2)	(35.0)	(139.7)	(105.3)
7	−153.4	147.8	185.9	388.8	616.1	1634.7	3587.2	3823.5	3927.0
	(264.7)	(20.3)	(3.4)	(131.5)	(153.3)	(68.9)	(316.9)	(14.9)	(96.8)
8	−183.0	161.6	176.4	475.9	497.3	1637.3	3595.7	3823.1	(3925.8
	(267.4)	(12.1)	(3.0)	(105.7)	(187.6)	(68.2)	(290.3)	(14.0)	(94.5)
9	−170.4	−103.9	90.8	131.0	323.3	1650.8	3718.1	3823.8	3911.8
	(14.3)	(23.4)	(0.0)	(211.8)	(331.9)	(114.0)	(22.77)	(9.2)	(60.5)
10	−199.0	92.2	235.8	335.6	342.8	1643.3	3729.2	3808.3	3905.9
	(164.3)	(44.6)	(182.7)	(166.5)	(60.6)	(75.6)	(21.9)	(19.2)	(81.7)
11	136.0	196.2	292.5	302.5	464.2	1646.5	3756.3	3801.8	3895.1
	(56.3)	(0.2)	(387.3)	(154.8)	(17.1)	(72.7)	(30.9)	(20.0)	(84.8)
H_2O						1639.4		3820.8	3922.7
						(71.1)		(7.5)	(61.8)
OH							3717.4		
							(14.6)		

(structure **9**, Fig. 4). For this structure, the singly occupied orbitals are located perpendicular to the molecular plane and the electronic state symmetry is $^2B_1$. The calculation is performed at higher levels of theory in this investigation. The optimized geometries at the UB3LYP/6-311++G(2*D*,2*P*) level are shown in Figure 4. The hydrogen bond distance (2.6 Å) is longer than those of all other H_3O_2 structures, indicating that the hydrogen bond is weak; consequently, the interaction energy is smaller than those of other structures (see Table I), although two hydrogen bonds are involved. However, it can be seen from Table II that there are two imaginary harmonic vibrational frequencies for structure **9**; it may be implied that this structure is not a transition state, which is inconsistent with result of Ref. [16]. Therefore, no further investigation at a higher level of theory was performed later.

For this system, a more reasonable form of hydrogen bonding has been revealed by using a higher level of theory, in which the water molecule donates two equivalent hydrogen bonds to the two lone pairs of the oxygen atom in OH moiety, together with OH moiety donating a hydrogen bond to the lone pairs of the oxygen atom in the water molecule at the same time (structures **10** and **11**; see Fig. 5). Structure **11** was fully optimized using the BLYP, B1LYP, B3LYP, and G96LYP methods with 6-311++g(2*d*,2*p*) and 6-311++g(3*df*,2*p*) basis sets. According to the singly occupied orbital, the electronic-state symmetries of structures **10** and **11** are characterized as $^2A'$. The hydrogen bond distances (2.2–2.4 Å) are longer than all of the H_3O_2 structures except for structure **9**, indicating weaker hydrogen bonding. Consequently, the interaction energy is smaller than those of some structures but larger than that of structures **3**, **4**, **6**, and **9**, in that three hydrogen bonds are involved, including one primary hydrogen bond (σ-type hydrogen bond) and two secondary hydrogen-bond interaction (double π-type hydrogen bond) which lead to bend of the primary hydrogen bond O···H—O [29]. According to structures **1–11**, the vibrational frequencies and vibrational modes are given in Table II; there is one imaginary harmonic vibration frequency for structure **10**, which implies that this structure is a tran-

TABLE III

Harmonic vibrational frequencies (in cm^{-1}) and their IR intensities (in km/mol).

Mode description	Symmetry	Frequencies	IR intensities
Structure **4**			
OH_2 stretching	A'	3912	110
OH_2 stretching	A'	3811	53
OH stretching	A'	3728	27
OH_2 scissors	A'	1647	67
H···OH bending (oop)	A''	386	198
H···OH bending (in plane)	A'	163	44
H···OH stretching	A'	114	0
H···OH bending (oop)	A''	6	24
H···OH bending (in plane)	A'	i218	179
Structure **10**			
OH_2 stretching	A''	3906	82
OH_2 stretching	A'	3808	19
· OH stretching	A'	3729	22
OH_2 scissors	A'	1643	76
OH_2 wag	A'	343	61
OH···OH_2 torsion	A''	336	167
H···OH stretching	A'	236	183
OH_2 rock	A''	92	45
OH_2 wag	A'	i199	164
Structure **11**			
OH_2 stretching	A''	3895	85
OH_2 stretching	A'	3802	20
· OH stretching	A'	3756	31
OH_2 scissors	A'	1646	73
OH_2 wag	A'	464	17
OH···OH_2 torsion	A''	302	155
O···H stretching	A'	293	387
H···OH bend	A'	196	0
OH_2 rock	A''	136	56

sition state. Following the normal mode of this imaginary frequency of structure **10** leads to structures **1** and **11**.

It is obvious that structure **1** is the most stable complex (globe minimum) due to its lowest energy (see Table I). There is a double π-type hydrogen bond between the O—H bonds of H_2O and the lone pairs on the O atom of the OH radical except for the O···H—O primary hydrogen bond [29]. Its bonding energy is 24.43 kJ/mol. This value is in agreement with Schaefer's calculation of 23.72 kJ/mol. Together with ZPE and TC at 298.15 K, structure **1** is still 7.45 kJ/mol, stable with respect to the isolated H_2O molecule and the OH radical. So, it may be predicted that complex **1** can be observed in high-resolution experiments. It can be estimated from Table I that, although the electronically excited $^2A''$ state (structure **2**) has a higher total energy than the $^2A'$ ground state (structure **1**), the energy splitting between the two states is so small (1.8 kJ/mol) that both states might be eventually observable. Complexes **3**, **4**, and **9** have the highest energy at the UB3LYP level of theory. The interaction energy lies in the range of −7.53 to −9.25 kJ/mol. After considering the ZPE and TC at 298.15 K, it is 0.96, −0.71, and −2.38 kJ/mol with respect to the isolated H_2O and OH, respectively. Therefore, structures **3**, **4**, and **9** are not candidates for experimental observation. In fact, they are transition states as the following frequency analysis shows. It is interesting to note that the energy of structures **7** and **8** rank the second in stability; after considering the ZPE and TC at 298.15 K, the interaction energies are −11.17 and −9.5 kJ/mol, respectively, the most stable in all of the complexes with respect to H_2O and OH. However, both are transition states on the potential energy hypersurface. So, they are not likely to be observed. The interaction

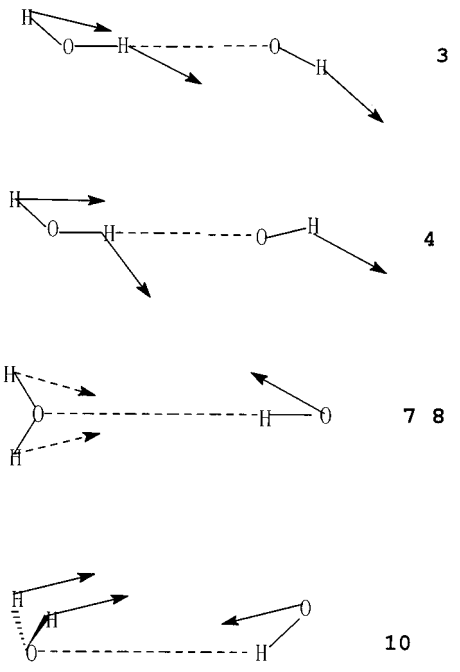

FIGURE 6. Imaginary vibration frequency mode of structures **3**, **4**, **7**, **8**, and **10**.

energy of structure **11** is 1.8 kJ/mol lower than that of structure **10**. However, after considering ZPE and TC at 298.15 K, it is about 4.18 kJ/mol higher than that of structure **10** to be only −2.92 kJ/mol. So, it can be predicted that structure **11** is less likely to be observable in high-resolution experiments.

IR SPECTRUM

The harmonic vibrational frequencies and IR intensities for structures **1–11** are shown in Table II. The IR spectra of structures **1**, **2**, and **6** have been discussed previously [16, 17] and will be discussed here only briefly. Both structures **1** and **2** have real vibrational frequencies, and so they are genuine minima. It can be seen from Table II that structures **1** and **2** have similar IR spectra, in accordance with their similar geometry parameters and total energies. We can see that both structures **3** and **4** have an imaginary frequency to be 164.3 and 217.7 cm^{-1}, respectively, corresponding to the O· · ·HO bending (in plane) (see Table III); this implies that they are not a true minimum but a transition state. Following the mode of the imaginary frequency (see Fig. 6), we obtain structure **6**. It can also be seen that there is an imaginary vibrational frequency to be 153.4 and 183.0, respectively, for structures **7** and **8** at the present level of theory, corresponding to the OH_2 wagging mode. Following such an imaginary mode from both structures **7** and **8** (see Fig. 6), we obtained two minima (structures **1** and **2**). So, they do not correspond to minima on the potential energy hypersurface and thus are not expected to be observable in the laboratory. In addition, there is an imaginary frequency to be 199.0 in structure **10**, corresponding to the OH_2 rocking mode (see Table III). Following the normal mode of the imaginary frequency, structure **10** connects structures **11** and **1** as IRC calculation shows (see Fig. 6). Structure **11** is shown in Table II to have real vibrational frequencies, and they are true minima. It is noteworthy that structure **9** is verified not to be a transition state at the UB3LYP/6-31++G(2D,2P) level of theory, in disagreement with Ref. [16].

To make a comparison with the vibrational frequency of the isolated water molecule and hydroxyl radical, the frequency shifts between the isolated molecules and these complexes are listed in Table IV. Because the frequency shifts are relatively stable with respect to theoretical methods, one can estimate the IR spectrum for the $H_2O \cdot HO$ system by combining the observed fundamental vibrational frequency of its moieties and the frequency shift in Table IV. The context of the $H_2O \cdot HO$ vibrational frequencies should be strictly analogous studies of the isolated H_2O and OH. Moreover, the fundamentals most likely to be observed in the laboratory may be the counterparts of those already character-

TABLE IV

Frequency shifts (in cm^{-1}) of structures 1–11 with respect to the monomers H_2O molecule and the OH radical.

Complex	OH stretching	H_2O asymmetrical stretching	H_2O symmetrical stretching	H_2O bending
1	−155.6	−6.6	−5.2	0.1
2	−158.8	−9.9	−6.2	4.0
6	−12.5	−24.3	−72.2	9.4
11	38.9	−27.6	−19.0	7.1

TABLE V

Harmonic vibrational frequencies (cm^{-1}) predicted for the $H_2O \cdot HO$ complex.

Complex	OH stretching	H_2O asymmetrical stretching	H_2O symmetrical stretching	H_2O bending
1	3414.4	3749.4	3651.8	1595.1
2	3411.2	3746.1	3650.8	1599.0
6	3557.5	3731.7	3584.8	1604.4
11	3608.9	3728.4	3638.0	1602.1
Exp.	3570	3756	3657	1595

ized precisely for isolated H_2O and OH. So, it can be predicted that the IR spectrum for the $H_2O \cdot OH$ system are obtained by combining the observed fundamental vibrational frequency of its moieties and the frequency shift in Table IV. Some predictions pertinent to the future observation of the fundamental IR spectrum of $H_2O \cdot HO$ are given in Table V. Hereafter, we will mainly discuss our predicted IR spectrum for structure **11** at the UB3LYP/6-311++G(2D,2P) level of theory employed, regarded as the more likely observable complex and revealed for the first time in this work.

According to the figures given in Table II, structure **11** has a different vibrational frequency from structures **1**, **2**, and **6**. The strongest bond of the infrared spectrum is at 292.5 cm^{-1} with an intensity of 387.3 km/mol, corresponding to the O···H stretching. Comparing with the isolated OH radical, the vibrational frequency and IR intensity rise by 38.9 cm^{-1} and 16.3 km/mol, respectively. ω_6, ω_8, and ω_9 correspond to the three vibrational modes of the H_2O group. It is obvious that for both the asymmetrical and symmetrical stretching modes of H_2O red shifts occur. The bending mode exhibits a small blue shift, typical for a hydrogen bond complex. The IR intensities of the three modes are similar to those of the isolated H_2O molecule. For the remaining four modes related to hydrogen bonding, there are three strong IR bonds corresponding to OH_2 rocking (136 cm^{-1}), $H_2O\cdots HO$ torsion (302.5 cm^{-1}), and OH_2 wagging (464.2 cm^{-1}). The weakest IR band is assigned to the H···OH bending mode. These predicted IR spectral characteristics might be confirmed by high-resolution IR spectroscopy.

From the observed fundamental vibrational frequencies of H_2O (3657, 1595, and 3756 cm^{-1}) [30] and OH (3570 cm^{-1}) [31] and the most reliable $H_2O \cdot HO$ frequency shifts predicted in this work, it may be predicted that the fundamentals of $H_2O \cdot OH$ complexes is shown in Table V. The fundamentals of both structures **1** and **6** have been predicted previously [15, 16], and structure **2** has a similar feature comparable to OH and H_2O to structure **1** due to their similar geometry and energy; therefore, the fundamental frequencies of structure **11** mainly are estimated here. The OH stretching fundamental frequency is predicted at 3609 cm^{-1} with roughly twice the IR intensity of that observed for the isolated OH radical. The fundamental frequency of the asymmetrical OH_2 stretching is predicted at 3728 cm^{-1} and with stronger IR intensity than that observed for water. The fundamental frequency of the symmetrical OH_2 stretching is predicted at 3638 cm^{-1} and has an IR intensity at least three times greater than that observed for the isolated H_2O molecule. Finally, the fundamental frequency of the water bending in the $H_2O \cdot OH$ complex is predicted at 1599 cm^{-1} with almost the same IR intensity as that of water. We look forward to these characteristics confirmed by high-resolution IR spectroscopy.

The rotational constant for structures **1**, **2**, **6**, and **11** are reported in Table VI. It is evident that spectroscopically structures **1**, **2**, **6**, and **11** will almost behave like prolate symmetrical rotors due to $B_A \gg B_B \approx B_C$. Because these complexes have permanent dipole moments as listed in Table III, they should be active in the microwave region of the spectra.

TABLE VI

Rotational constants (in Mhz) and dipole moments (in debye) for the $H_2O \cdot HO$ complexes calculated using B3LYP methods with the 6-311++g(2*d*,2*p*) basis set.

Complexes	Rotational constants			Dipole moment
	B_A	B_B	B_C	
1	353,412	6847	6760	4.0380
2	337,763	6728	6651	3.9540
6	322,862	6617	6484	1.1718
11	195,262	9908	9860	0.2862

This information is useful in characterizing their rotational and rovibrational spectra.

ACKNOWLEDGMENTS

This work is supported by the Natural Science Foundation of Shantung Province (Y99B01), the State Key Laboratory Foundation of Crystal Material, and the National Natural Science Foundation of China (2967305).

References

1. Aloisio, S.; Francisco, J. S. J Phys Chem A 1998, 102, 1899.
2. Aloisio, S.; Francisco, J. S. J Phys Chem A 1999, 103, 6049.
3. Wang, B.; Hou, H.; Gu, Y. J Mol Struct Theochem 2000, 505, 241.
4. Wang, B.; Hou, H.; Gu, Y. Chem Phys Lett 1999, 309, 274.
5. Legon, A. C.; Millen, D. J. Chem Rev 1986, 86, 635.
6. Legon, A. C.; Millen, D. J. Acc Chem Res 1987, 20, 39.
7. Legon, A. C. Chem Phys Lett 1995, 237, 291.
8. Cooke, S. A.; Corlett, G. K.; Evans, C. M.; Legon, A. C. Chem Phys Lett 1997, 272, 61.
9. Legon, A. C. Chem Phys Lett 1997, 279, 55.
10. Kollman, P.; In: Scheafer, H. F., Ed. Modern Theoretical Chemistry. Vol. 4. Plenum: New York, p 153, 1977.
11. Hobza, P.; Zahradnik, R. Intermolecular Complex. The Role of van der Waals Systems in Physical Chemistry and Biodisciplines. Elsevier: Amsterdam, 1988.
12. Mijoule, C.; Latajka, Z.; Bordis, D. Chem Phys Lett 1993, 210, 279.
13. Hobza, P.; Sponer, J.; Beschel, T. J Comput Chem 1995, 16, 1315.
14. Lundell, J.; Latajka, Z. J Phys Chem 1997, 101, 5004.
15. Kim, K. S.; Kim, H. S.; Jang, J. H.; Mhin, B. J.; Xie, Y.; Schaefer, H. F. J Chem Phys 1991, 94, 2057.
16. Xie, Y.; Schaefer, H. F. J Chem Phys 1993, 98, 8829.
17. Wang, B.; Hou, H.; Gu, Y. Chem Phys Lett 1999, 303, 96.
18. Becke, A. D. J Chem Phys 1993, 98, 1372.
19. Lee, C.; Yang, W.; Parr, R. G. Phys Rev B 1988, 37, 785.
20. Boys, S. F.; Bernardi, F. Mol Phys 1970, 19, 553.
21. Kim, K.; Jordan, K. D. J Phys Chem 1994, 98, 10089.
22. Novoa, J. J.; Sosa, C. J Phys Chem 1995, 99, 15837–15845.
23. Zhou, Z.; Fu, A.; Du, D. Int J Quantum Chem 2000, 78, 186.
24. Raghavachari, K.; Trucks, G. W.; Pople, J. A.; Head-Gordon, M. Chem Phys Lett 1989, 157, 479.
25. Tsuzuki, S.; Uchimaru, T.; Tanabe, K. Chem Phys Lett 1998, 286, 202–208.
26. Gonzalez, C.; Schlegel, H. B. J Chem Phys 1989, 90, 2154.
27. Gonzalez, C.; Schlegel, H. B. J Phys Chem 1990, 94, 5523.
28. Frisch, M. J.; Trucks, G. W.; Schlegel, H. B.; Gill, P. W. M.; Johnson, B. G.; Robb, M. A.; Cheeseman, J. R.; Keith, T. A.; Petersson, G. A.; Montgomery, J. A.; Raghavachari, K.; Allaham, M. A.; Zakrzewski, V. G.; Ortiz, J. V.; Foresman, J. B.; Cioslowski, J.; Stefanov, B. B.; Nanayakkara, A.; Challacombe, M.; Peng, C. Y.; Ayala, P. Y.; Chen, W.; Wong, M. W.; Andres, J. L.; Replogle, E. S.; Gomperts, R.; Martin, R. L.; Fox, D. J.; Binkley, J. S.; Defrees, D. J.; Baker, J.; Stewart, J. P.; Head-Gordon, M.; Gonzales, C.; Pople, J. A. Gaussian 94, revision E.1. Gaussian, Inc.: Pittsburgh, PA, 1995.
29. Li, Z.; Wu, D.; Li, Z.; Huang, X.; Fu, T.; Sun, C. J Phys Chem A 2001, 105, 1163.
30. Benedict, W. S.; Gailar, N.; Plyler, E. K. J Chem Phys 1956, 24, 1139.
31. Maillard, J. P.; Chauville, J.; Mantz, A. W. J Mol Spectrosc 1976, 63, 120.